

Calibration of MODIS-based gross primary production over an alpine meadow on the Tibetan Plateau

Gang Fu, Zhenxi Shen, Xianzhou Zhang, Peili Shi, Yongtao He, Yangjian Zhang, Wei Sun, Jianshuang Wu, Yuting Zhou, and Xu Pan

Abstract. Moderate-resolution imaging spectroradiometer (MODIS) gross primary production (GPP) was compared with estimated GPP (GPP_EC) from eddy covariance measurements over an alpine meadow on the Tibetan Plateau in 2005–2007. The MODIS GPP (GPP_MOD17A2) with a bias of $-0.38 \text{ g C m}^{-2} \text{ d}^{-1}$ (i.e., about -40.58% of the mean of the GPP_EC) strongly underestimated the GPP_EC for the alpine meadow. The MODIS GPP was recalibrated using measured surface meteorological data, including photosynthetically active radiation (PAR), daily minimum air temperature (T_{amin}) and daytime mean vapor pressure deficit (VPD), revised fractional photosynthetically active radiation (FPAR), and the revised maximum light use efficiency (LUE_{max}) of 0.81 g C MJ^{-1} (compared with the default value of 0.68 g C MJ^{-1} for grassland in the MODIS GPP algorithm) for the alpine meadow. The MODIS-based FPAR was about 14.70% larger than the surface-estimated FPAR using surface-measured leaf area index (LAI) data. Additionally, the temporal resolution of surface-measured LAI data was relatively low. Therefore, the linear relationship between surface-measured LAI and MODIS-based LAI was established ($R^2 > 0.80$, $P < 0.001$). Then the revised MODIS LAI datasets were used to calculate the revised FPAR. The revised LUE_{max} was optimized from the MOD17A2 algorithm using daily surface measurements, including LAI, PAR, VPD, T_{amin} and GPP_EC. The calibrated MOD17A2 algorithm could explain 88% of GPP_EC variance for the alpine meadow. The bias between GPP_MOD17A2 and calculated GPP from the MOD17A2 algorithm using surface-measured PAR, T_{amin} , and VPD, MODIS-based FPAR, and the default LUE_{max} of 0.68 g C MJ^{-1} was $-0.17 \text{ g C m}^{-2} \text{ d}^{-1}$ (i.e., about -17.60% of the mean of the GPP_EC). The underestimation of LUE_{max} caused a 13.78% underestimation of GPP. In contrast, the overestimation of FPAR resulted in a 7.17% overestimation of GPP. The net effect of meteorology data and FPAR resulted in a 13.84% underestimation of GPP. These results showed that MODIS-based meteorology data, FPAR, and LUE_{max} for the alpine meadow needed to be adjusted.

Résumé. La production primaire brute (PPB) dérivée des données de MODIS (Moderate-Resolution Imaging Spectroradiometer) a été comparée avec des valeurs de PPB (PPB_CT) estimées à l'aide de la méthode des corrélations turbulentes au-dessus d'une prairie alpine sur le plateau tibétain en 2005–2007. Les données PPB de MODIS (PPB_MOD17A2) avec un biais de $-0,38 \text{ g C m}^{-2} \text{ d}^{-1}$ (c.-à-d. environ $-40,58\%$ de la moyenne des valeurs de PPB_CT) ont fortement sous-estimé les valeurs de PPB_CT pour la prairie alpine. La PPB de MODIS a été ré-étalonnée en utilisant des données météorologiques de surface incluant le rayonnement photosynthétiquement actif (PAR), la température minimale journalière de l'air (T_{amin}) et le déficit diurne moyen de pression de vapeur (DPV), la fraction du rayonnement photosynthétiquement actif révisée (FPAR) et l'efficacité d'utilisation maximale de la lumière révisée (LUE_{max}) de $0,81 \text{ g C MJ}^{-1}$ (comparativement à la valeur par défaut de $0,68 \text{ g C MJ}^{-1}$ pour les prairies dans l'algorithme de la PPB de MODIS) pour la prairie alpine. Le rayonnement FPAR dérivé des données de MODIS était approximativement de $14,70\%$ plus élevé que le FPAR estimé en surface (FPAR_Sur) à l'aide des données LAI mesurées en surface. De plus, la résolution temporelle des données LAI mesurées en surface était relativement faible. Ainsi, la relation linéaire entre le LAI mesuré en surface et le LAI basé sur MODIS était préalablement établie ($R^2 > 0,80$, $P < 0,001$). Ensuite, l'ensemble des données révisées LAI de MODIS a été utilisé pour calculer les valeurs révisées de FPAR. Les valeurs révisées de LUE_{max} ont été optimisées à partir de l'algorithme MOD17A2 en utilisant les mesures journalières de surface incluant LAI, PAR, DPV, T_{amin} et PPB_CT. L'algorithme MOD17A2 étalonné permettait d'expliquer 88% de

Received 22 July 2011. Accepted 21 March 2012. Published on the Web at <http://pubs.casi.ca/journal/cjrs> on 13 June 2012.

Gang Fu, Zhenxi Shen,¹ Xianzhou Zhang, Peili Shi, Yongtao He, Yangjian Zhang, Wei Sun, Jianshuang Wu, and Yuting Zhou. Lhasa Plateau Ecosystem Research Station, Key Laboratory of Ecosystem Network Observation and Modeling, Institute of Geographic Sciences and Natural Resources Research, Beijing 100101, China.

Gang Fu, Jianshuang Wu, Yuting Zhou, and Xu Pan. Graduate University of Chinese Academy of Sciences, Beijing 100049, China.

Xu Pan. Institute of Botany, Chinese Academy of Sciences, Beijing 100093, China.

¹Corresponding author (e-mail: shenzx@igsnr.ac.cn).

la variance de PPB_CT pour la prairie alpine. Le biais entre la PPB_MOD17A2 et la PPB calculée (PPB_MOD1) à partir de l'algorithme MOD17A2 en utilisant le PAR mesuré en surface, T_{amin} et DPV, la FPAR basée sur les données de MODIS et la valeur par défaut de LUE_{max} de $0,68 \text{ g C MJ}^{-1}$ était de $-0,17 \text{ g C m}^{-2} \text{ d}^{-1}$ (c.-à-d. approximativement $-17,60\%$ de la moyenne de la PPB_CT). La sous-estimation de LUE_{max} a engendré une sous-estimation de $13,78\%$ de la PPB. Par contre, la surévaluation de FPAR a résulté en une surévaluation de $7,17\%$ de la PPB. L'effet net des données météorologiques et de FPAR a résulté en une sous-estimation de $13,84\%$ de la PPB. Ces résultats ont montré la nécessité d'ajuster les données météorologiques dérivées de MODIS, FPAR et LUE_{max} pour la prairie alpine.

[Traduit par la Rédaction]

Introduction

Photosynthesis is a key step in the carbon sequestration of terrestrial ecosystems, and is closely linked to growth, respiration, and litter fall (Mäkelä et al., 2006). A major challenge in quantifying the global carbon cycle is quantification predicting gross primary production (GPP) at a variety of spatial and temporal scales (Yuan et al., 2007). The light use efficiency (LUE) model has some potential to adequately address the spatial and temporal dynamics of GPP (Yuan et al., 2007; Wu et al., 2009). The LUE model proposes that biological production is directly proportional to the amount of absorbed photosynthetically active radiation (APAR) by the vegetation canopy (Monteith 1972, 1977; Running et al., 2004). Many LUE models have been developed to calculate net primary production or GPP, such as the Carnegie, Ames, Stanford Approach (Potter et al., 1993), the Global Production Efficiency Model (Prince and Goward 1995), and the Vegetation Production Model (Xiao et al., 2004).

Moderate-resolution imaging spectroradiometer (MODIS) is being used to continuously monitor GPP routinely from space (Running et al., 2004; Coops et al., 2007b). The MODIS GPP algorithm is also based on the LUE model (Zhao et al., 2005; Gebremichael and Barros 2006; Heinsch et al., 2006; Zhang et al., 2008). It provides an 8 day composite product of GPP of 1 km spatial resolution at the global scale (Heinsch et al., 2003). However, it is necessary to test the validity of the MODIS GPP using local surface-measured data (Heinsch et al., 2006; Zhang et al., 2008). The eddy covariance (EC) technique provides one of the best approaches to calculate GPP of ecosystems (Yuan et al., 2007; Wu et al., 2009), so EC-based GPP is often used to validate the MODIS GPP (Turner et al., 2003, 2005, 2006a, 2006b; Zhao et al., 2005; Gebremichael and Barros 2006; Heinsch et al., 2006; Coops et al., 2007a, 2007b; Zhang et al., 2008). There is a trend in the MODIS GPP products toward an overestimation of GPP at low productivity sites because of an overestimation of the fraction of photosynthetically active radiation (FPAR) absorbed by the canopy and an underestimation at high productivity sites because of an underestimation of vegetation LUE (Turner et al., 2006a). The mean annual GPP from MOD17 are lower than surface-estimated mean annual GPP for an alpine meadow site and a cropland site mainly because the MOD17A algorithm underestimates maximum LUE for the two vegetation types (Zhang et al., 2008). Although leaf area index (LAI) and FPAR of Collection 5 is more accurate, MODIS GPP of this

Collection results in a much larger bias than earlier Collections in comparison with EC-based GPP for a tropical savanna site (Kanniah et al., 2009). MODIS GPP gives satisfactory results during the wet season, but causes overestimation in comparison with EC-based GPP during the dry season over a tropical wet-dry savanna in northern Queensland (Leuning et al., 2005). The mean MODIS GPP is about 30% lower than the mean EC-based GPP over a temperate Douglas fir forest (Coops et al., 2007b).

In China, alpine meadows cover about $6.4 \times 10^5 \text{ km}^2$ and are concentrated in the western and southwestern regions, most on the Tibetan Plateau, containing 35.4 Pg of carbon (i.e., 26.4% of total carbon in grassland of China) (Ni, 2002). Previous studies showed that alpine meadows might be a carbon sink if the carbon lost due to grazing was not significant (Kato et al., 2004). Hence, alpine meadows play a very important role in the regional carbon budget in China (Zhang et al., 2008). Additionally, with atmospheric CO_2 concentration increasing, the GPP of alpine meadows on the Tibetan Plateau might increase if the precipitation does not change and alpine meadows can sequester more carbon (Xu et al., 2005, 2007). However, few studies have been conducted to test the validity of MODIS-based GPP of alpine meadows on the Tibetan Plateau. Therefore, the calibration was done over an alpine meadow in the Tibetan Autonomous Region.

The objectives of this study were to (i) evaluate the MODIS-based GPP (GPP_MOD17A2) using EC-based GPP and (ii) calibrate the GPP_MOD17A2 using the continuously measured surface meteorological data and LAI, and revised maximum light use efficiency (LUE_{max}).

Methods

Site description

The study site (91.07°E , 30.50°N , 4333 m above sea level) is located in Damxung Grassland Observation Station, Tibetan Autonomous Region in China, where an EC tower as a part of ChinaFlux was established in July 2003. The annual average sunlight is 2880.9 h and the annual average solar radiation is 7527.6 MJ m^{-2} . Annual mean air temperature is 1.3°C , with minimum monthly mean of -10.4°C in January and maximum monthly mean of 10.7°C in July. Annual average precipitation is around 476.8 mm while the annual potential evapotranspiration is about 1725.7 mm. The soil is frozen from November to January of the following year.

The soil texture is sandy loam. The vegetation around the site is C3-dominated alpine meadow. The dominant species are *Kobresia pygmaea*, *Stipa capillacea*, and *Carex montis-everestii*. The vegetation in the area starts to turn green in May, reaches maximum biomass during the period of July or August, and then senesces in October.

Eddy covariance measurements and meteorological data

Fluxes of carbon dioxide and water vapor have been continuously measured with a fetch of at least 200 m from all directions (Xu et al., 2007) since 2003. The EC system, installed at the height of 2.1 m above the ground, consisted of an open-path fast-response infrared gas analyzer (IRGA, Model LI7500, Li-Cor Inc., Lincoln, Neb.) and a three-dimensional sonic anemometer (Model CSAT3, Campbell Scientific Inc., Logan, Utah).

Along with the measurements of CO₂ and H₂O flux, routine meteorological data and soil parameters were also simultaneously measured. This included relative humidity and air temperature at the height of 1.5 m and 2.1 m (Model HMP45C, Vaisala, Helsinki, Finland); actual vapor pressure, atmospheric pressure (CS105, Vaisala Inc.); wind direction (Model W200P, Vector); wind speed (Model A100R, Vector); precipitation (Model 52203, RM Young Inc.); photosynthetically active radiation (LI190SB, Li-cor Inc.); soil temperature at the depths of 0.05, 0.1, 0.2, 0.5, and 0.8 m (Model 107-L, Campbell Scientific Inc.); soil surface average tem-

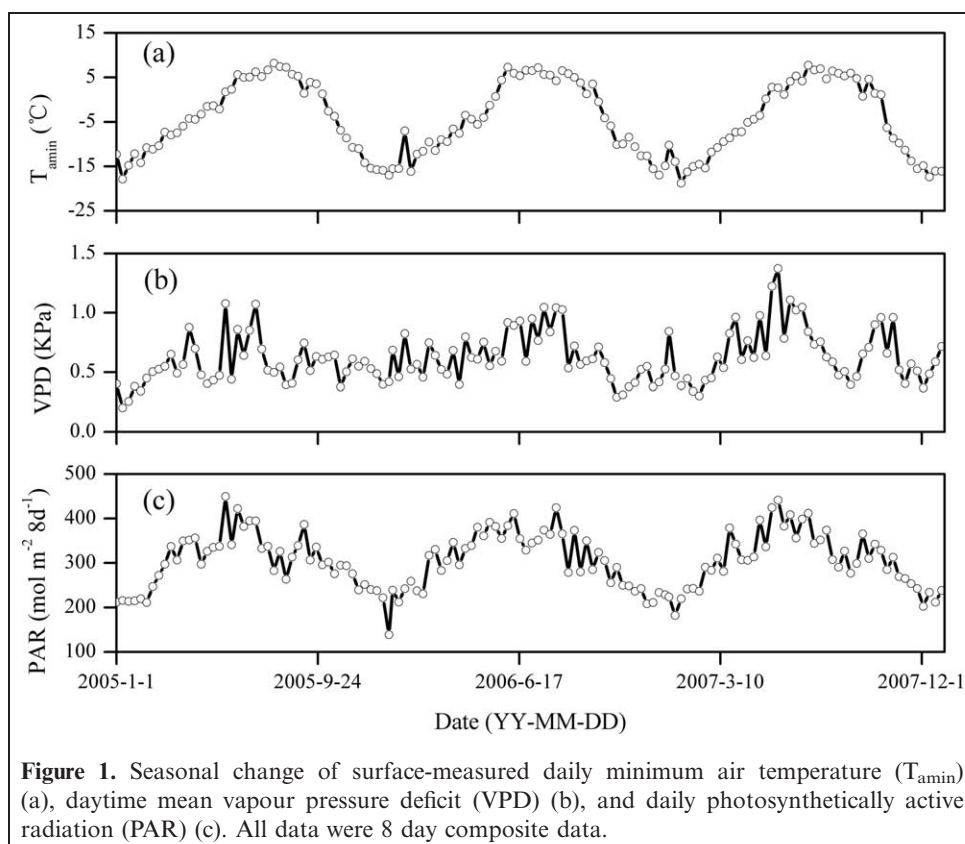
perature at depths from 0 to 0.06 m (Model TCAV, Campbell Scientific); soil volumetric water content at the depths of 0.05, 0.1 and 0.5 m (Model CS616-L, Campbell Scientific Inc.); and land surface temperature (Model IRTS-P, APOGEE). Vapor pressure deficit (VPD) was calculated as the difference between the saturation and actual vapor pressures at the given temperature based on the measured relative humidity and air temperature (Yu et al., 2008).

These data were recorded as half-hourly average values with a data-logger (Model CR23XTD, Campbell Scientific Inc.) except the precipitation which was recorded as an hour total amount. A more detailed description of EC and other meteorological parameter measurements are given in Xu et al. (2005, 2007) and Yu et al. (2008).

Seasonal changes of an 8 day composite daily minimum air temperature (T_{amin}), daytime VPD and daily photosynthetically active radiation (PAR) in 2005–2007 are illustrated in **Figure 1**.

LAI measurement and surface-based FPAR calculation

LAI was measured with a leaf area meter (Model AM200, ADC BioScientific Ltd.) during the growing season (from May to mid-October) about every half month in 2005–2007. On each measurement day, five 50 cm × 50 cm replicate plots were randomly set within the fetch of EC tower (Fu et al., 2009). Such LAI data were only available on the measurement days. Therefore, the MODIS 8 day composite



LAI products with a 1 km spatial resolution (MOD15A2) were used to estimate consecutive LAI data to obtain fine temporal resolution integrated LAI data. The linear relationship between surface-measured LAI and MODIS-based LAI was established in this study ($R^2 > 0.80$, $P < 0.001$, $n = 19$). Then the MODIS-based LAI and the linear relationship were used to estimate the integrated LAI data. In this study, the revised FPAR were calculated using the integrated LAI data with a Beer–Lambert law as follows (Ruimy et al., 1999):

$$\text{FPAR} = 0.95 \times (1 - \exp(-k \times \text{LAI})) \quad (1)$$

where k is the light extinction coefficients it was assumed to be 0.5, which was the same as the default value in the MODIS algorithm (Zhang et al., 2008).

On average, MODIS-based FPAR (FPAR_MOD) was about 14.70% higher than the calculated FPAR from Equation (1) using surface-measured LAI across the three consecutive growing seasons when surface-measured LAI was available (Figure 2). Therefore, MODIS-based FPAR was revised as the approach mentioned previously.

Gap filling and EC-based GPP calculation

The nonlinear regression method (Falge et al., 2001) was used to fill diurnal and nocturnal gaps. The missing diurnal flux data were estimated from the Michaelis–Menten equation with a 10 day moving window.

$$\text{NEE}_d = \frac{\alpha \text{PPFD} \text{GPP}_{\max}}{\alpha \text{PPFD} + \text{GPP}_{\max}} - R_d \quad (2)$$

where NEE_d ($\mu\text{mol CO}_2 \text{ m}^{-2} \text{ s}^{-1}$) and R_d ($\mu\text{mol CO}_2 \text{ m}^{-2} \text{ s}^{-1}$) are the net ecosystem exchange and ecosystem respiration during the daytime period, respectively. PPFD is the photosynthetic photon flux density ($\mu\text{mol quantum m}^{-2} \text{ s}^{-1}$), α is the ecosystem apparent quantum yield or maximum light

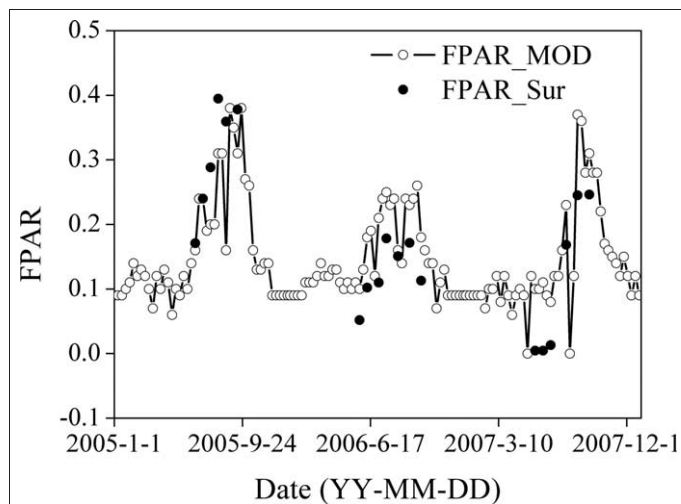


Figure 2. Seasonal change of surface-estimated fractional photosynthetically active radiation using surface-measured leaf area index (FPAR_Sur) and MOD15A2 FPAR (FPAR_MOD).

use efficiency ($\mu\text{mol CO}_2 \mu\text{mol}^{-1} \text{PPFD}$), and GPP_{\max} is the asymptotic GPP at saturating light ($\mu\text{mol CO}_2 \text{ m}^{-2} \text{ s}^{-1}$).

For nocturnal missing data, the Lloyd and Taylor (1994) equation was used as follows:

$$R_n = R_{\text{ref}} \exp \left[E_0 \left(\frac{1}{T_{\text{ref}} - T_0} - \frac{1}{T_k - T_0} \right) \right] \quad (3)$$

where R_n is nocturnal ecosystem respiration, i.e., NEE_n , R_{ref} stands for the ecosystem respiration rate at the reference temperature of 10°C , E_0 represents temperature sensitivity of ecosystem respiration, and T_k ($^\circ\text{C}$) is soil temperature at the depth of 0.05 m.

Gap-filled half-hourly data were used to calculate the EC-based GPP (i.e., GPP_{EC}).

$$\text{GPP} = \text{NEE}_d + R_d \quad (4)$$

The nocturnal fitted equation (Equation 3) between R_n and soil temperature at the depth of 0.05 m was extrapolated to estimate the R_d .

Only the GPP_{EC} of the alpine meadow from 1 May to 15 October (i.e., the vegetation growing season) was calculated by means of this approach and the GPP_{EC} during other periods (i.e., the vegetation nongrowing season) was set to be zero.

MOD17A2 algorithm and MODIS data

The MOD17A2 algorithm was presented in detail in previous studies (Zhao et al., 2005; Gebremichael and Barros 2006; Heinsch et al., 2006; Zhang et al., 2008) and the MOD17 user's guide (Heinsch et al., 2003). Therefore, only a brief description is given here. The MOD17A2 GPP algorithm is based on a LUE approach (Heinsch et al., 2003; Gebremichael and Barros 2006; Turner et al., 2006a; Coops et al., 2007a).

LUE is combined with estimated APAR to calculate GPP (kg C day^{-1}) as follows:

$$\text{GPP} = \text{LUE} \times \text{APAR} \quad (5)$$

where APAR stands for the absorbed PAR by vegetation canopy. APAR can be calculated as:

$$\text{APAR} = \text{PAR} \times \text{FPAR} \quad (6)$$

where FPAR, i.e., the fraction of absorbed PAR by vegetation canopy, is derived from the MOD15A2 product, which is an 8 day composite LAI/FPAR MODIS product at 1 km spatial resolution (Myneni et al., 2002; Yang et al., 2006; Olofsson and Eklundh 2007). The incident PAR can be estimated by incident shortwave radiation (SWRad).

$$\text{PAR} = 0.45 \times \text{SWRad} \quad (7)$$

LUE is calculated as

$$\text{LUE} = \text{LUE}_{\max} \times \text{TMIN}_{\text{scalar}} \times \text{VPD}_{\text{scalar}} \quad (8)$$

where LUE_{max} is the maximum light use efficiency or the ecosystem apparent quantum yield ($kg\ C\ MJ^{-1}$), and $TMIN_scalar$ and VPD_scalar are the two attenuation scalars with a range from 0 to 1.

The original MODIS-based GPP (MOD17A2 product) at the spatial resolution of 1 km was called GPP_MOD17A2 in this study. GPP_MOD1, GPP_MOD2, and GPP_MOD3 were all calculated from the MOD17A2 algorithm. GPP_MOD1 was calculated using surface-measured meteorology data, including PAR, T_{amin} and VPD, and MOD15A2 FPAR, whereas GPP_MOD2 and GPP_MOD3 were both calculated using surface-measured PAR, T_{amin} and VPD, and surface-based FPAR. The default parameters (Table 1) were used to calculate GPP_MOD1 and GPP_MOD2. The same default parameters, except for LUE_{max} (Table 1), were used to calculate GPP_MOD3.

Determination of surface-based LUE_{max}

LUE_{max} varies with vegetation types (Xiao et al., 2004; Coops et al., 2007b, 2009), stand structure, and vegetation coverage (Xu et al., 2007). However, there should be an individual LUE_{max} for an individual stand (Gower et al., 1999; Xu et al., 2007). LUE_{max} can be retrieved from an analysis of the ratio of GPP to APAR and the attenuation factors of LUE_{max} (Zhang et al., 2008). In this study, the surface-based LUE_{max} (i.e., revised LUE_{max}) was determined from the MOD17A2 algorithm using daily inputs of surface-measured VPD, T_{amin} and APAR, and EC-based GPP at the following stages: surface-measured VPD and T_{amin} were used to calculate the moisture and temperature attenuation scalars (VPD_scalar and $TMIN_scalar$) of LUE_{max} , respectively; and surface-measured LAI were used to calculate the surface-estimated FPAR through Equation (1). Then, surface-estimated FPAR and surface-measured PAR were used to calculate the surface-based APAR; and the linear equation ($y = 0.81x$, $R^2 = 0.747$, $P < 0.001$, $n = 19$), where y and x represent EC-based GPP and the multiplicative of APAR and $TMIN_scalar$ and VPD_scalar , respectively, was calculated as mentioned

previously. Therefore, the surface-based LUE_{max} was set to be $0.81\ g\ C\ MJ^{-1}$ in this study.

Statistical analysis

The root mean squared error (RMSE) and bias were used to analyze the correspondence between the estimated GPP from EC measurements and the modeled GPP from the MOD17A2 algorithm:

$$RMSE = \sqrt{\frac{1}{n} \sum_{i=1}^n (y_{predicted} - y_{measured})^2} \quad (9)$$

$$Bias = \sum_{i=1}^n (y_{predicted} - y_{measured}) / n \quad (10)$$

where n is the number of observations and i is the observation number.

Results

The seasonal changes of GPP_EC, GPP_MOD17A2, GPP_MOD1, GPP_MOD2, and GPP_MOD3 from 2005 to 2007 are presented in Figure 3. There were similar seasonal changes among GPP_EC, GPP_MOD17A2, GPP_MOD1, GPP_MOD2, and GPP_MOD3. The peak values of GPP_MOD17A2 and GPP_MOD2 were lower than those of GPP_EC for all three consecutive growing seasons, whereas those of GPP_MOD1 were only lower in 2005 and 2007. In contrast, the peak values of GPP_MOD3 were higher than those of GPP_EC in 2005 and 2006, but lower in 2007.

The differences among GPP_EC, GPP_MOD17A2, GPP_MOD1, GPP_MOD2, and GPP_MOD3 varied through time (Table 2, Figure 3). The annual GPP_MOD17A2 was only 57.84%, 77.32%, and 48.62% of the annual GPP_EC in 2005, 2006, and 2007, respectively. Although the annual GPP_MOD1 was about 20.80%–38.55% higher than the annual GPP_MOD17A2, it was only about 62.76%–93.40% of the annual GPP_EC. The annual GPP_MOD2 was about 5.85%–9.18% lower

Table 1. Values for fractional photosynthetically active radiation (FPAR), meteorology data, maximum light use efficiency (LUE_{max} , $g\ C\ MJ^{-1}$), T_{amin_max} ($^{\circ}C$), T_{amin_min} ($^{\circ}C$), VPD_{max} (KPa), and VPD_{min} (KPa) used in gross primary production (GPP) calculation*.

GPP	FPAR	Meteorology data	LUE_{max}	T_{amin_max}	T_{amin_min}	VPD_{max}	VPD_{min}
GPP_MOD17A2	MOD15A2 FPAR	DAO [†]	0.68	12.02	-8.00	3.5	0.65
GPP_MOD1	MOD15A2 FPAR	Surface-measured	0.68	12.02	-8.00	3.5	0.65
GPP_MOD2	Surface-based FPAR [‡]	Surface-measured	0.68	12.02	-8.00	3.5	0.65
GPP_MOD3	Surface-based FPAR [‡]	Surface-measured	0.81	12.02	-8.00	3.5	0.65

* T_{amin_max} , the upper limit value of the daily minimum air temperature; T_{amin_min} , the lower limit value of the daily minimum air temperature; VPD_{max} , the upper limit value of daytime mean vapor pressure deficit; VPD_{min} , the lower limit value of daytime mean vapor pressure deficit.

[†]DAO, NASA's Data Assimilation Office.

[‡]To obtain consecutive surface-based FPAR, the linear relationship between surface-measured leaf area index (LAI) and MODIS-based LAI was firstly established. Then the MODIS-based LAI and the linear relationship were used to estimate the surface-based consecutive LAI dataset. Lastly the surface-based consecutive LAI dataset was used to calculate the consecutive surface-based FPAR from Equation (1).

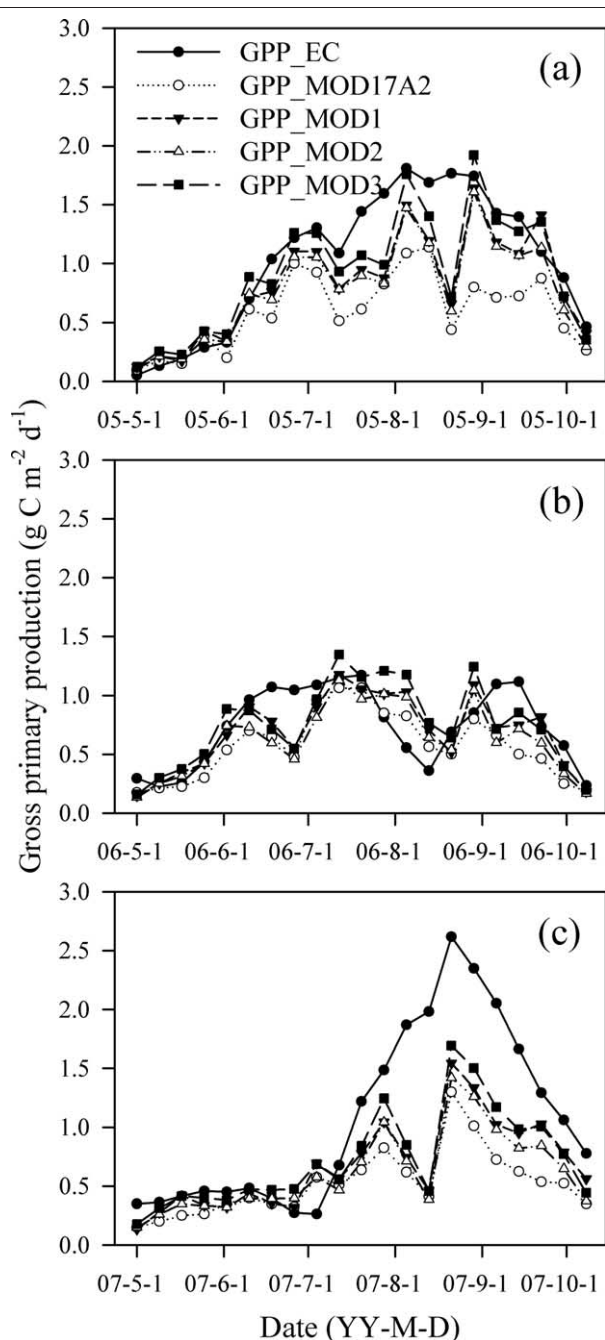


Figure 3. Seasonal change of estimated gross primary production from eddy covariance measurements (GPP_EC), MODIS-Terra 8 day composite GPP (GPP_MOD17A2), calculated GPP (GPP_MOD1) from the MOD17A2 algorithm using default parameters (Table 1), surface-measured meteorological data (i.e., photosynthetically active radiation, daily minimum air temperature, and daytime mean vapour pressure deficit), and MODIS-based FPAR, calculated GPP (GPP_MOD2) from the MOD17A2 algorithm using default parameters (Table 1) and surface-measured meteorological data and surface-based FPAR data and calculated GPP (GPP_MOD3) from the MOD17A2 algorithm using surface-measured meteorological data, surface-based FPAR data, and the revised maximum light use efficiency of 0.81 g C MJ^{-1} (Table 1) in 2005 (a), 2006 (b), and 2007 (c).

than the annual GPP_MOD1. The annual GPP_MOD3 was 9.90% and 31.95% lower in 2005 and 2007, respectively, than the annual GPP_EC, but 1.62% higher in 2006.

Annual GPP_MOD17A2, GPP_MOD1, GPP_MOD2, and GPP_MOD3 had a consistent decreasing trend from 2005 to 2007 (Table 2). In contrast, annual GPP_EC decreased in the order $2007 > 2005 > 2006$ (Table 2). Therefore, the annual variation trends of photosynthetically active radiation, air temperature, vapor pressure deficit, soil water content, and precipitation across the full growing season were not consistent with gross primary production. In detail, the mean daily maximum and minimum air temperatures were 14.69 and 3.54, 15.85 and 3.60, and 16.35 and 3.77 °C in 2005, 2006, and 2007, respectively. The daily mean air temperature was 8.70, 9.34, and 9.80 °C in 2005, 2006, and 2007, respectively. The mean PAR was 42.89, 43.99, and 44.49 $\text{mol m}^{-2} \text{day}^{-1}$ in 2005, 2006, and 2007, respectively. The total amount of precipitation was 467.2, 211.7, and 411.3 mm in 2005, 2006, and 2007, respectively, whereas mean soil water content at the depth of 0.05 m was 0.147, 0.098, and 0.117 $\text{m}^3 \text{m}^{-3}$, respectively. In contrast, mean daytime VPD was 0.62, 0.76, and 0.80 kPa, in 2005, 2006, and 2007, respectively.

The comparisons between GPP_MOD1, GPP_MOD2, GPP_MOD3, and GPP_MOD17A2 are illustrated in Figure 4. GPP_MOD1 was larger than GPP_MOD17A2 with a linear slope of 1.276, an R^2 of 0.966, and an RMSE of $0.152 \text{ g C m}^{-2} \text{d}^{-1}$. GPP_MOD2 was also higher than GPP_MOD17A2 with a linear slope of 1.184, an R^2 of 0.964, and an RMSE of $0.144 \text{ g C m}^{-2} \text{d}^{-1}$. Additionally, the linear slope between GPP_MOD3 and GPP_MOD17A2 was 1.413 with an R^2 of 0.964 and an RMSE of $0.172 \text{ g C m}^{-2} \text{d}^{-1}$. The mean biases of GPP_MOD1, GPP_MOD2, GPP_MOD3, and GPP_MOD17A2 were 0.17, 0.11, and 0.24 $\text{g C m}^{-2} \text{d}^{-1}$, which were about 17.60%, 11.57%, and 25.35% of the mean of GPP_EC, respectively.

Figure 5 describes the linear relationships between GPP_EC and GPP_MOD17A2, GPP_MOD1, GPP_MOD2, and GPP_MOD3. GPP_MOD17A2, GPP_MOD1, GPP_MOD2, and GPP_MOD3 significantly explained 86.7%, 88.6%, 88.0%, and 88.0% temporal variation of GPP_EC, respectively. However, the linear slopes were 0.527, 0.692, 0.640, and 0.764, respectively. The mean biases of GPP_MOD17A2, GPP_MOD1, GPP_MOD2, GPP_MOD3, and GPP_EC were -0.38 , -0.22 , -0.27 and $-0.14 \text{ g C m}^{-2} \text{d}^{-1}$, which were about -40.58% , -22.98% , -29.01% , and -15.23% of the mean of GPP_EC, respectively. These figures indicated that the underestimation of LUE_{max} caused a 13.78% underestimation of GPP. In contrast, the overestimation of FPAR resulted in a 7.17% overestimation. Additionally, the net effect of LUE_{max} and FPAR caused a 7.75% underestimation, whereas the overall effect of meteorology data and FPAR resulted in a 13.84% underestimation.

Table 2. Annual total GPP ($\text{g C m}^{-2} \text{y}^{-1}$) comparisons among estimated GPP (GPP_EC) from eddy covariance measurements, MODIS GPP product (GPP_MOD17A2), GPP_MOD1, GPP_MOD2, and GPP_MOD3.

Year	GPP_EC	GPP_MOD17A2	GPP_MOD1*	GPP_MOD2†	GPP_MOD3‡
2005	173.23	100.20	138.82	130.70	156.07
2006	123.78	95.70	115.60	105.33	125.78
2007	180.05	87.55	112.99	102.62	122.53

*Calculated GPP from MOD17A2 algorithm using default parameters, surface-measured meteorological data (i.e., photosynthetically active radiation, daily minimum air temperature and daytime mean vapor pressure deficit and MODIS-based FPAR (Table 1).

†Calculated GPP from MOD17A2 algorithm using default parameters and surface-measured meteorological data and surface-based FPAR data (Table 1).

‡Calculated GPP from MOD17A2 algorithm using surface-measured meteorological data, surface-based FPAR data and revised maximum light use efficiency (Table 1).

Discussion

GPP

The annual GPP_EC in this study was $173.23 \text{ g C m}^{-2} \text{y}^{-1}$ in 2005, which was slightly different from some previous studies that were made in the same alpine meadow site (Hu et al., 2008; Fu et al., 2009). Hu et al. (2008) presented that the annual GPP_EC was $167.65 \text{ g C m}^{-2} \text{y}^{-1}$, whereas Fu et al. (2009) showed that the annual GPP_EC was $173.7 \text{ g C m}^{-2} \text{y}^{-1}$ in 2005. The difference between GPP_EC in the current study and previous studies might be attributed to three types of errors: the determination of growing season, the usage of different gap filling equations, and the determination of the parameters in the gap filling equation.

The mean annual GPP_EC for the alpine meadow in this study was $159.02 \pm 30.71 \text{ g C m}^{-2} \text{y}^{-1}$ in 2005–2007, which was much lower than annual GPP_EC for the alpine meadow of the Haibei EC measurements site (Hu et al., 2008; Zhang et al., 2008; Fu et al., 2009). Fu et al. (2009) and Hu et al. (2008) presented that the annual GPP_EC in Haibei were 553.9 and $580.37 \text{ g C m}^{-2} \text{y}^{-1}$ in 2005, respectively. Zhang et al. (2008) showed that the annual GPP_EC was 503.9 and $604.7 \text{ g C m}^{-2} \text{y}^{-1}$ in 2002 and 2003, respectively. The probable reasons why mean annual GPP_EC in the Damxung site was much lower than that in the Haibei site were: (i) lower vegetation cover (it was larger than 80% in Haibei while lower than 50% in Damxung (Fu et al., 2009)); (ii) lower canopy height (it was about 55–70 cm in Haibei while lower than 10 cm in Damxung (Fu et al., 2009)); (iii) lower soil water content (Hu et al., 2008; Fu et al., 2009); (iv) higher VPD (Hu et al., 2008; Fu et al., 2009); and (v) lower LAI. For example, accumulated LAI during the growing season in 2005 were 70.8 and $225.5 \text{ m}^2 \text{m}^{-2}$ in Damxung and Haibei, respectively (Fu et al., 2009).

The biases between MODIS-based GPP and EC-based GPP were -0.43 , -0.17 , and $-0.55 \text{ g C m}^{-2} \text{d}^{-1}$ in 2005, 2006, and 2007, respectively, while the daily mean values of EC-based GPP were 1.03 , 0.74 , and $1.07 \text{ g C m}^{-2} \text{d}^{-1}$ in 2005, 2006, and 2007, respectively. This finding showed there may be a trend that the larger the daily mean of the GPP_EC, the larger the bias.

The annual GPP_MOD17A2 were equivalent to 57.84%, 77.32%, and 48.62% of the annual GPP_EC in 2005, 2006, and 2007, respectively. This result was consistent with a previous calibration study that showed the annual GPP from Collection 4 MOD17A2 accounted for 1/2–2/3 of the annual GPP_EC for alpine meadow (Zhang et al., 2008). Therefore, Collection 4 and Collection 5 MOD17A2 GPP both underestimated GPP for alpine meadow ecosystems on the Tibetan Plateau.

Meteorology data

The MOD17A2 GPP algorithm is based on NASA's Data Assimilation Office (DAO) meteorology data (Heinsch et al., 2003). To date, many studies have confirmed that NASA's DAO meteorology data could produce large errors in the GPP algorithm (Zhao et al., 2005; Gebremichael and Barros 2006; Heinsch et al., 2006). Zhao et al. (2005) presented that the average relative error of the difference between DAO and EC-based meteorology data was 27% ($\pm 45\%$). Heinsch et al. (2006) presented that the error between annual GPP computed from DAO and EC-based meteorology data was 28%. The relative biases between the GPP estimated using DAO and EC-based meteorology data were -77% and $+18\%$ for a mixed forest site in the humid tropics and an open shrubland site in a semiarid region, respectively (Gebremichael and Barros 2006). Comparisons between MODIS-based GPP and calculated GPP from the MOD17A2 algorithm using MODIS-based FPAR, surface-measured meteorology data and the default LUE_{max} of 0.68 g C MJ^{-1} showed that the bias between GPP estimates using DAO data and surface-measured meteorology data was $-0.17 \text{ g C m}^{-2} \text{d}^{-1}$ (i.e., about -17.60% of the mean of GPP_EC), which implied that the DAO meteorology data was coarse for the alpine meadow.

FPAR

MODIS-based FPAR overestimated surface-estimated FPAR in this study, which was in line with some previous studies (Fensholt et al., 2004; Turner et al., 2005). Nevertheless, other studies presented that MODIS-based FPAR

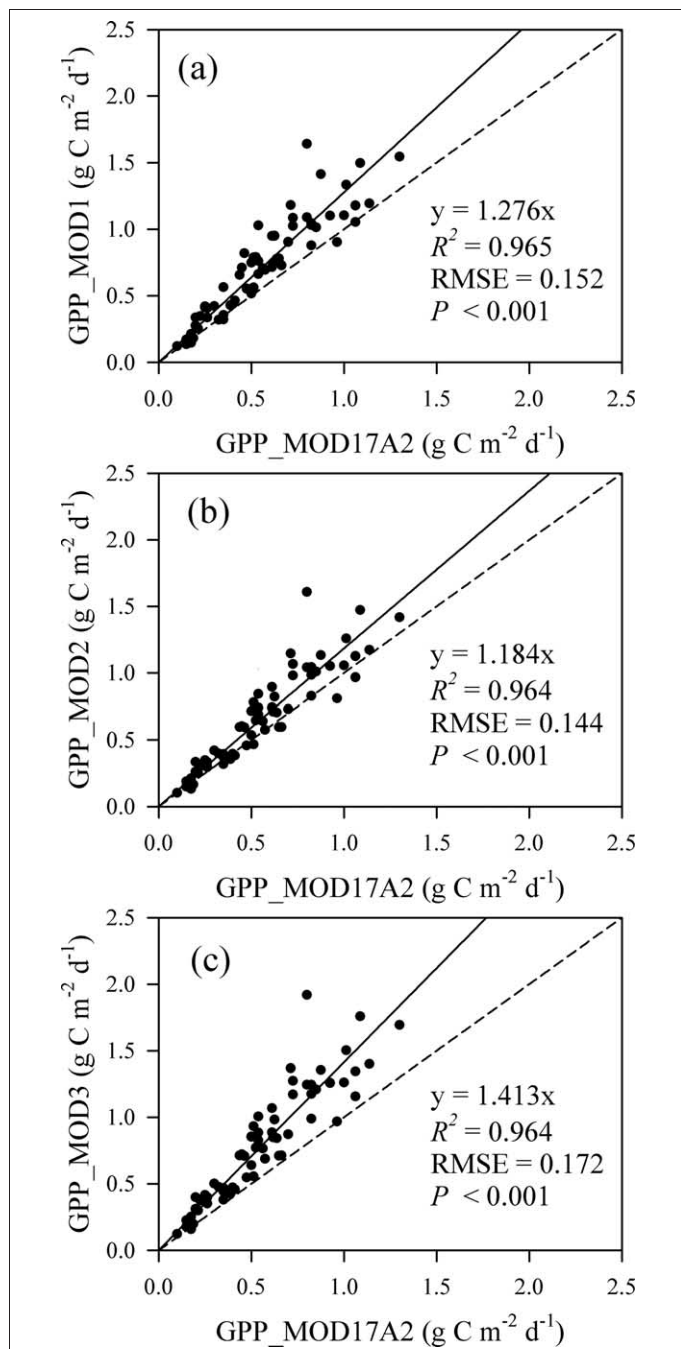


Figure 4. Comparisons between MODIS GPP product (GPP_MOD17A2) and calculated GPP (GPP_MOD1) from the MOD17A2 algorithm using default parameters (Table 1), surface-measured meteorological data (i.e., photosynthetically active radiation, daily minimum air temperature, and daytime mean vapour pressure deficit) and MODIS-based FPAR and calculated GPP (GPP_MOD2) from the MOD17A2 algorithm using default parameters (Table 1) and surface-measured meteorological data and surface-based FPAR data and calculated GPP (GPP_MOD3) from the MOD17A2 algorithm using surface-measured meteorology data, surface-based FPAR and the revised maximum light use efficiency of 0.81 g C MJ^{-1} (Table 1), respectively. Dash lines indicate 1:1 reference lines.

was lower than the surface-measured FPAR (Olofsson and Eklundh 2007; Zhang et al., 2008). Additionally, good agreement between MODIS-based FPAR and surface-measured FPAR was also observed in previous studies (Zhang et al., 2008). Olofsson and Eklundh (2007) presented that the canopy densities might explain the different comparison results between MODIS-based FPAR and surface-based FPAR. In their study, they thought the MODIS-based FPAR might approach the maximum FPAR level for highly closed canopies which could result in underestimation or good agreement with surface-based FPAR. In contrast, they pointed out the overestimation of surface-based FPAR could be attributed to the fact that the canopies were sparse. The vegetation of the alpine meadow was sparse with low LAI in this study, which might explain the result that surface-estimated FPAR was lower than MODIS-based FPAR.

LUE_{max}

The revised LUE_{max} was nearly equivalent to the maximum apparent quantum use efficiency of 0.85 g C MJ^{-1} under low-light conditions (Xu et al., 2007), but lower than the maximum apparent quantum use efficiency of 1.30 g C MJ^{-1} under full-light conditions (Xu et al., 2005). This indicated that GPP might be dampened under high light at the ecosystem level.

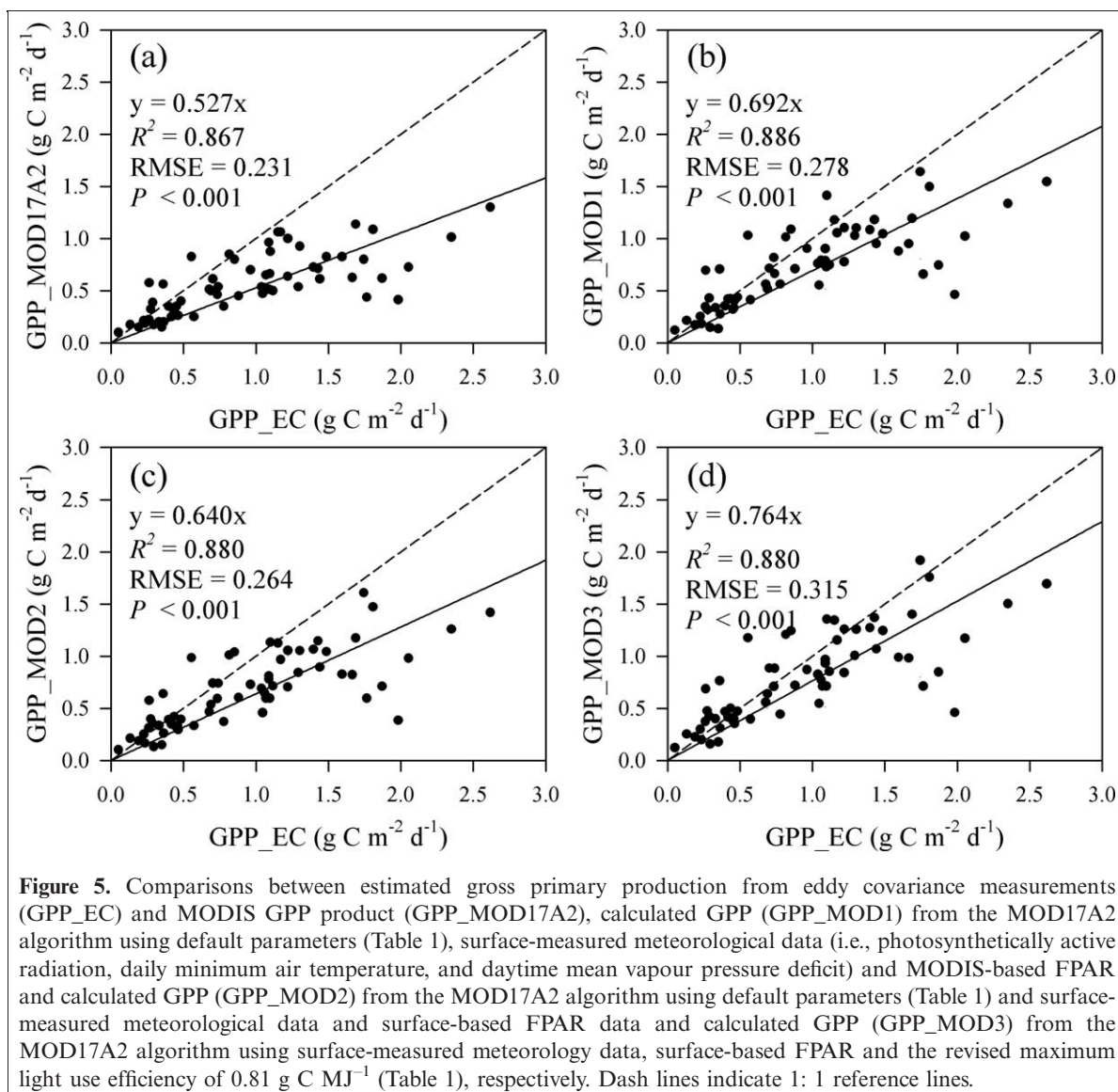
The revised LUE_{max} was 0.81 g C MJ^{-1} for the alpine meadow in this study, which was 19.12% larger than the default value of 0.68 g C MJ^{-1} for grassland. Previous studies confirmed that the default LUE_{max} for grassland underestimated the LUE_{max} for an alpine meadow on the Tibetan Plateau (Zhang et al., 2008). Taken together, the default LUE_{max} of 0.68 g C MJ^{-1} for grassland should be adjusted for alpine meadows on the Tibetan Plateau.

The value of LUE_{max} is obtained from the biome properties look-up table in the MOD17A2 GPP algorithm which is dependent on MODIS land cover classification, i.e., MOD12Q1 (Heinsch et al., 2003). Nevertheless, there is one type for grassland in MOD17A2 GPP algorithm. Therefore, the vegetation type classification of MOD12Q1 is coarse for grassland in China because there are 18 grassland types in China (Ni, 2002). LUE_{max} varies with vegetation types (Xiao et al., 2004; Coops et al., 2007b, 2009), so the 18 grassland types may have their own LUE_{max}.

Calibrated MODIS algorithm

The GPP based on the calibrated MODIS algorithm (i.e., GPP_MOD3) linearly explained 88% variations of the GPP_EC, whereas it was still 15.2% lower than the GPP_EC. The bias between the GPP_MOD3 and GPP_EC was probably attributed to the following conditions.

(i) The default parameters in the MODIS algorithm (Table 1) that would not be very suitable for the alpine meadow in this study. The maximum values of daytime



mean vapor pressure deficit and daily minimum air temperature were 1.37 kPa and 8.19°C across the three consecutive growing seasons, which were much lower than the default maximum values of 3.5 kPa and 12.02°C in the MODIS algorithm. Therefore, the calculated temperature and water attenuation scalars using default parameters of the MODIS algorithm may result in errors for the alpine meadow. For example, the calculated water attenuation scalars from the MODIS algorithm were still at a high level (higher than 0.86) during the growing season in 2006, whereas the annual precipitation in 2006 was only about 50% of the annual mean precipitation (i.e., 476.8 mm). This indicated that the water attenuation scalar may not adequately reflect the negative effect of drying on GPP in 2006.

(ii) The vapor pressure deficit may not be a good indicator of soil water content and precipitation, and thereby it does not adequately reflect the effect of water availability on GPP. Although the precipitation during the growing season in 2006 was much lower than that in 2005 and 2007, the mean

water attenuation scalar in 2006 was not strongly different from that in 2005 and 2007. Daily precipitation and soil water content and daytime vapor pressure deficit could linearly explain 26.9%, 53.3%, and 12.5% variations of GPP_EC with RMSE values of 0.512 , 0.409 , and $0.560 \text{ g C m}^{-2} \text{ d}^{-1}$ across the three consecutive growing seasons, respectively ($P < 0.01$). This implied that it might be better that soil water content or precipitation was used to be the water attenuation parameter for the alpine meadow instead of the vapor pressure deficit. Additionally, vapor pressure deficit may have exaggerated the negative effect of drying on GPP_EC in 2007.

(iii) There were errors in estimating daytime ecosystem respiration using the relationship between nocturnal ecosystem respiration and soil temperature. Generally, daytime soil temperature is higher in comparison with nighttime soil temperature and the temperature sensitivity of ecosystem respiration decreases with increasing temperature (Jassal et al., 2007). Therefore, daytime and nighttime respiration

may have different responses to soil temperature and consequently the extrapolation approach probably caused error. Moreover, leaf respiration in light is relatively low in comparison with darkness (Hoefnagel et al., 1998). This could overestimate daytime canopy respiration and thereby GPP (Janssens et al., 2001; Wohlfahrt et al., 2005).

Conclusions

In this study, MODIS-based GPP was evaluated by surface-estimated GPP from EC measurements over an alpine meadow on the Tibetan Plateau. FPAR_MOD was compared with the surface-estimated FPAR (FPAR_Sur) using surface-measured LAI. Additionally, surface-measured LAI was used to calibrate MODIS-based LAI. The calibrated MODIS LAI dataset was used to calculate the revised FPAR.

GPP_MOD17A2 with a bias of $-0.38 \text{ g C m}^{-2} \text{ d}^{-1}$ (i.e., about -40.58% of the mean of the GPP_EC) strongly underestimated the GPP_EC for the alpine meadow. The revised LUE_{max} was 0.81 g C MJ^{-1} (compared with the default value of 0.68 g C MJ^{-1} for grassland in the MODIS GPP algorithm) for the alpine meadow. The FPAR_MOD was about 14.70% larger than the FPAR_Sur. The calibrated MOD17A2 algorithm could explain 88% of GPP_EC variance for the alpine meadow. The 16.05% underestimation of LUE_{max} caused a 13.78% underestimation of GPP. In contrast, the overestimation of FPAR resulted in a 7.17% overestimation of GPP.

Acknowledgements

This work was funded by the National Science and Technology Plan Project of China (Nos. 2006BAC01A04 and 2007BAC06B01), National Basic Research Program of China (2010CB833500), and National Natural Science Foundation of China (Nos. 41171084 and 40771121).

References

Coops, N.C., Black, T.A., Jassal, R.P.S., Trofymow, J.A.T., and Morgenstern, K. 2007a. Comparison of MODIS, eddy covariance determined and physiologically modeled gross primary production (GPP) in a Douglas-fir forest stand. *Remote Sensing of Environment*, Vol. 107, No. 3, pp. 385–401. doi: 10.1016/j.rse.2006.09.010.

Coops, N.C., Jassal, R.S., Leuning, R., Black, A.T., and Morgenstern, K. 2007b. Incorporation of a soil water modifier into MODIS predictions of temperate Douglas-fir gross primary productivity: Initial model development. *Agricultural and Forest Meteorology*, Vol. 147, Nos. 3–4, pp. 99–109. doi: 10.1016/j.agrformet.2007.07.001.

Coops, N.C., Ferster, C.J., Waring, R.H., and Nightingale, J. 2009. Comparison of three models for predicting gross primary production across and within forested ecoregions in the contiguous United States. *Remote Sensing of Environment*, Vol. 113, No. 3, pp. 680–690. doi: 10.1016/j.rse.2008.11.013.

Falge, E., Baldocchi, D., Olson, R., Anthoni, P., Aubinet, M., Bernhofer, C., Burba, G., Ceulemans, R., Clement, R., Dolman, H., Granier, A., Gross, P., Grünwald, T., Hollinger, D., Jensen, N.O., Katul, G., Keronen, P., Kowalski, A., Lai, C.T., Law, B.E., Meyers, T., Moncrieff, J., Moors, E., Munger, J.W., Pilegaard, K., Rannik, Ü., Rebmann, C., Suyker, A., Tenhunen, J., Tu, K., Verma, S.S., Vesala, T., Wilson, K., and Wofsy, S. 2001. Gap filling strategies for defensible annual sums of net ecosystem exchange. *Agricultural and Forest Meteorology*, Vol. 107, No. 1, pp. 43–69. doi: 10.1016/S0168-1923(00)00225-2.

Fensholt, R., Sandholt, I., and Rasmussen, M.S. 2004. Evaluation of MODIS LAI, fAPAR, and the relation between fAPAR and NDVI in a semi-arid environment using in situ measurements. *Remote Sensing of Environment*, Vol. 91, Nos. 3–4, pp. 490–507. doi: 10.1016/j.rse.2004.04.009.

Fu, Y., Zheng, Z., Yu, G., Hu, Z., Sun, X., Shi, P., Wang, Y., and Zhao, X. 2009. Environmental influences on carbon dioxide fluxes over three grassland ecosystem in China. *Biogeosciences*, Vol. 6, No. 12, pp. 2879–2893. doi: 10.5194/bg-6-2879-2009.

Gebremichael, M., and Barros, A.P. 2006. Evaluation of MODIS gross primary productivity (GPP) in tropical monsoon regions. *Remote Sensing of Environment*, Vol. 100, No. 2, pp. 150–166. doi: 10.1016/j.rse.2005.10.009.

Gower, S.T., Kucharik, C.J., and Norman, J.M. 1999. Direct and indirect estimation of leaf area index, fAPAR, and net primary production of terrestrial ecosystems. *Remote Sensing of Environment*, Vol. 70, No. 1, pp. 29–51. doi: 10.1016/S0034-4257(99)00056-5.

Heinsch, F.A., Reeves, M., Votava, P., Kang, S.Y., Milesi, C., Zhao, M.S., Glassy, J., Jolly, W.M., Loehman, R., Bowker, C.F., Kimball, J.S., Nemani, R.R., and Running, S.W. 2003. User's guide, GPP and NPP (MOD17A2/A3) products, NASA MODIS land algorithm [online]. Available from <http://www.ntsg.umd.edu/modis/MOD17UsersGuide.pdf> [accessed 31 December 2009].

Heinsch, F.A., Zhao, M.S., Running, S.W., Kimball, J.S., Nemani, R.R., Davis, K.J., Bolstad, P.V., Cook, B.D., Desai, A.R., Ricciuto, D.M., Law, B.E., Oechel, W.C., Kwon, H., Luo, H.Y., Wofsy, S.C., Dunn, A.L., Munger, J.W., Baldocchi, D.D., Xu, L.K., Hollinger, D.Y., Richardson, A.D., Stoy, P.C., Siqueira, M.B.S., Monson, R.K., Burns, S.P., and Flanagan, L.B. 2006. Evaluation of remote sensing based terrestrial productivity from MODIS using regional tower eddy flux network observations. *IEEE Transactions on Geoscience and Remote Sensing*, Vol. 44, No. 7, pp. 1908–1925. doi: 10.1109/TGRS.2005.853936.

Hoefnagel, M.H.N., Atkin, O.K., and Wiskich, J.T. 1998. Interdependence between chloroplasts and mitochondria in the light and the dark. *Biochimica Et Biophysica Acta-Bioenergetics*, Vol. 1366, No. 3, pp. 235–255. doi: 10.1016/S0005-2728(98)00126-1.

Hu, Z.M., Yu, G.R., Fu, Y.L., Sun, X.M., Li, Y.N., Shi, P.L., Wang, Y.F., and Zheng, Z.M. 2008. Effects of vegetation control on ecosystem water use efficiency within and among four grassland ecosystems in China. *Global Change Biology*, Vol. 14, No. 7, pp. 1609–1619. doi: 10.1111/j.1365-2486.2008.01582.x.

Jassal, R.S., Black, T.A., Cai, T.B., Morgenstern, K., Li, Z., Gaumont-Guay, D., and Nesci, Z. 2007. Components of ecosystem respiration and an estimate of net primary productivity of an intermediate-aged Douglas-fir stand. *Agricultural and Forest Meteorology*, Vol. 144, Nos. 1–2, pp. 44–57. doi: 10.1016/j.agrformet.2007.01.011.

Janssens, I.A., Lankreijer, H., Matteucci, G., Kowalski, A.S., Buchmann, N., Epron, D., Pilegaard, K., Kutsch, W., Longdoz, B., Grünwald, T., Montagnani, L., Dore, S., Rebmann, C., Moors, E.J.,

- Grelle, A., Rannik, U., Morgenstern, K., Oltchev, S., Clement, R., Gudmundsson, J., Minerbi, S., Berbigier, P., Ibrom, A., Moncrieff, J., Aubinet, M., Bernhofer, C., Jensen, N.O., Vesala, T., Granier, A., Schulze, E.D., Lindroth, A., Dolman, A.J., Jarvis, P.G., Ceulemans, R., and Valentini, R. 2001. Productivity overshadows temperature in determining soil and ecosystem respiration across European forests. *Global Change Biology*, Vol. 7, No. 3, pp. 269–278. doi: 10.1046/j.1365-2486.2001.00412.x.
- Kanniah, K.D., Beringer, J., Hutley, L.B., Tapper, N.J., and Zhu, X. 2009. Evaluation of collection 4 and 5 of the MODIS gross primary productivity product and algorithm improvement at a tropical savanna site in northern Australia. *Remote Sensing of Environment*, Vol. 113, No. 9, pp. 1808–1822. doi: 10.1016/j.rse.2009.04.013.
- Kato, T., Tang, Y.H., Gu, S., Cui, X.Y., Hirota, M., Du, M.Y., Li, Y.N., Zhao, Z.Q., and Oikawa, T. 2004. Carbon dioxide exchange between the atmosphere and an alpine meadow ecosystem on the Qinghai-Tibetan Plateau, China. *Agricultural and Forest Meteorology*, Vol. 124, Nos. 1–2, pp. 121–134. doi: 10.1016/j.agrformet.2003.12.008.
- Leuning, R., Cleugh, H.A., Zegelin, S.J., and Hughes, D. 2005. Carbon and water fluxes over a temperate Eucalyptus forest and a tropical wet/dry savanna in Australia: measurements and comparison with MODIS remote sensing estimates. *Agricultural and Forest Meteorology*, Vol. 129, Nos. 3–4, pp. 151–173. doi: 10.1016/j.agrformet.2004.12.004.
- Lloyd, J., and Taylor, J.A. 1994. On the temperature dependence of soil respiration. *Functional Ecology*, Vol. 8, No. 3, pp. 315–323. doi: 10.2307/2389824.
- Mäkelä, A., Kolari, P., Karimäki, J., Nikinmaa, E., Perämäki, M., and Hari, P. 2006. Modelling five years of weather-driven variation of GPP in a boreal forest. *Agricultural and Forest Meteorology*, Vol. 139, Nos. 3–4, pp. 382–398.
- Monteith, J.L. 1972. Solar radiation and productivity in tropical ecosystems. *Journal of Applied Ecology*, Vol. 9, No. 3, pp. 747–766. doi: 10.2307/2401901.
- Monteith, J.L. 1977. Climate and the efficiency of crop production in Britain. *Philosophical Transactions of the Royal Society of London Series B-Biological Sciences*, Vol. 281, No. 980, pp. 277–294. doi: 10.1098/rstb.1977.0140.
- Myneni, R.B., Hoffman, S., Knyazikhin, Y., Privette, J.L., Glassy, J., Tian, Y., Wang, Y., Song, X., Zhang, Y., Smith, G.R., Lotsch, A., Friedl, M., Morisette, J.T., Votava, P., Nemani, R.R., and Running, S.W. 2002. Global products of vegetation leaf area and fraction absorbed PAR from year one of MODIS data. *Remote Sensing of Environment*, Vol. 83, Nos. 1–2, pp. 214–231. doi: 10.1016/S0034-4257(02)00074-3.
- Ni, J. 2002. Carbon storage in grasslands of China. *Journal of Arid Environments*, Vol. 50, No. 2, pp. 205–218. doi: 10.1006/jare.2001.0902.
- Olofsson, P., and Eklundh, L. 2007. Estimation of absorbed PAR across Scandinavia from satellite measurements. Part II: Modeling and evaluating the fractional absorption. *Remote Sensing of Environment*, Vol. 110, No. 2, pp. 240–251. doi: 10.1016/j.rse.2007.02.020.
- Potter, C.S., Randerson, J.T., Field, C.B., Matson, P.A., Vitousek, P.M., Mooney, H.A., and Klooster, S.A. 1993. Terrestrial ecosystem production: a process model-based on global satellite and surface data. *Global Biogeochemical Cycle*, Vol. 7, No. 4, pp. 811–841. doi: 10.1029/93GB02725.
- Prince, S.D., and Goward, S.N. 1995. Global primary production: a remote sensing approach. *Journal of Biogeography*, Vol. 22, Nos. 4–5, pp. 815–835. doi: 10.2307/2845983.
- Ruimy, A., Kergoat, L., Bondeau, A., and The Participants of the Potsdam NPP Model Intercomparison. 1999. Comparing global models of terrestrial net primary productivity (NPP): analysis of differences in light absorption and light-use efficiency. *Global Change Biology*, Vol. 5, No. S1, pp. 56–64. doi: 10.1046/j.1365-2486.1999.00007.x.
- Running, S.W., Nemani, R.R., Heinsch, F.A., Zhao, M.S., Reeves, M., and Hashimoto, H. 2004. A continuous satellite-derived measure of global terrestrial primary production. *Bioscience*, Vol. 54, No. 6, pp. 547–60. doi: 10.1641/0006-3568(2004)054[0547:ACSMOG]2.0.CO;2.
- Turner, D.P., Ritts, W.D., Cohen, W.B., Gower, S.T., Zhao, M.S., Running, S.W., Wofsy, S.C., Urbanski, S., Dunn, A.L., and Munger, J.W. 2003. Scaling gross primary production (GPP) over boreal and deciduous forest landscapes in support of MODIS GPP product validation. *Remote Sensing of Environment*, Vol. 88, No. 3, pp. 256–270. doi: 10.1016/j.rse.2003.06.005.
- Turner, D.P., Ritts, W.D., Cohen, W.B., Maieringer, T.K., Gower, S.T., Kirschbaum, A.A., Running, S.W., Zhao, M.S., Wofsy, S.C., Dunn, A.L., Law, B.E., Campbell, J.L., Oechel, W.C., Kwon, H.J., Meyers, T.P., Small, E.E., Kurc, S.A., and Gamon, J.A. 2005. Site-level evaluation of satellite-based global terrestrial gross primary production and net primary production monitoring. *Global Change Biology*, Vol. 11, No. 4, pp. 666–684. doi: 10.1111/j.1365-2486.2005.00936.x.
- Turner, D.P., Ritts, W.D., Cohen, W.B., Gower, S.T., Running, S.W., Zhao, M.S., Costa, M.H., Kirschbaum, A.A., Ham, J.M., Saleska, S.R., and Ahl, D.E. 2006a. Evaluation of MODIS NPP and GPP products across multiple biomes. *Remote Sensing of Environment*, Vol. 102, Nos. 3–4, pp. 282–292. doi: 10.1016/j.rse.2006.02.017.
- Turner, D.P., Ritts, W.D., Zhao, M.S., Kurc, S.A., Dunn, A.L., Wofsy, S.C., Small, E.E., and Running, S.W. 2006b. Assessing interannual variation in MODIS-based estimates of gross primary production. *IEEE Transactions on Geoscience and Remote Sensing*, Vol. 44, No. 7, pp. 1899–1907. doi: 10.1109/TGRS.2006.876027.
- Wohlfahrt, G., Bahn, M., Haslwanter, A., Newsely, C., and Cernusca, A. 2005. Estimation of daytime ecosystem respiration to determine gross primary production of a mountain meadow. *Agricultural and Forest Meteorology*, Vol. 130, Nos. 1–2, pp. 13–25. doi: 10.1016/j.agrformet.2005.02.001.
- Wu, C.Y., Niu, Z., Tang, Q., Huang, W.J., Rivard, B., and Feng, J.L. 2009. Remote estimation of gross primary production in wheat using chlorophyll-related vegetation indices. *Agricultural and Forest Meteorology*, Vol. 149, Nos. 6–7, pp. 1015–1021. doi: 10.1016/j.agrformet.2008.12.007.
- Xiao, X.M., Hollinger, D., Aber, J., Goltz, M., Davidson, E.A., Zhang, Q.Y., and Moore III, B. 2004. Satellite-based modeling of gross primary production in an evergreen needleleaf forest. *Remote Sensing of Environment*, Vol. 89, No. 4, pp. 519–534. doi: 10.1016/j.rse.2003.11.008.
- Xu, L.L., Zhang, X.Z., Shi, P.L., and Yu, G.R. 2005. Establishment of apparent quantum yield and maximum ecosystem assimilation on Tibetan Plateau alpine meadow ecosystem. *Science in China Series D-Earth Sciences*, Vol. 48, No. S1, pp. 141–147.
- Xu, L.L., Zhang, X.Z., Shi, P.L., Li, W.H., and He, Y.T. 2007. Modeling the maximum apparent quantum use efficiency of alpine meadow ecosystem on Tibet Plateau. *Ecological Modelling*, Vol. 208, Nos. 2–4, pp. 129–134. doi: 10.1016/j.ecolmodel.2007.05.013.
- Yang, W.Z., Huang, D., Tan, B., Stroeve, J.C., Shabanov, N.V., Knyazikhin, Y., Nemani, R.R., and Myneni, R.B. 2006. Analysis of leaf area index and fraction of PAR absorbed by vegetation products from the terra MODIS sensor: 2000–2005. *IEEE Transactions on Geoscience and*

Remote Sensing, Vol. 44, No. 7, pp. 1829–1842. doi: 10.1109/TGRS.2006.871214.

Yu, G.R., Zhang, L.M., Sun, X.M., Fu, Y.L., Wen, X.F., Wang, Q.F., Li, S.G., Ren, C.Y., Song, X., Liu, Y.F., Han, S.J., and Yan, J.H. 2008. Environmental controls over carbon exchange of three forest ecosystems in eastern China. *Global Change Biology*, Vol. 14, No. 11, pp. 2555–2571.

Yuan, W.P., Liu, S.G., Zhou, G.S., Zhou, G.Y., Tieszen, L.L., Baldocchi, D., Bernhofer, C., Gholz, H., Goldstein, A.H., Goulden, M.L., Hollinger, D.Y., Hu, Y.M., Law, B.E., Stoy, P.C., Vesala, T., Wofsy, S.C., and other AmeriFlux collaborators. 2007. Deriving a light use efficiency model from eddy covariance flux data for predicting daily gross primary production across biomes. *Agricultural and Forest*

Meteorology, Vol. 143, Nos. 3–4, pp. 189–207. doi: 10.1016/j.agrformet.2006.12.001.

Zhang, Y.Q., Yu, Q., Jiang, J., and Tang, Y.H. 2008. Calibration of Terra/MODIS gross primary production over an irrigated cropland on the North China Plain and an alpine meadow on the Tibetan Plateau. *Global Change Biology*, Vol. 14, No. 4, pp. 757–767. doi: 10.1111/j.1365-2486.2008.01538.x.

Zhao, M.S., Heinsch, F.A., and Nemani, R.R. 2005. Improvements of the MODIS terrestrial gross and net primary production global data set. *Remote Sensing of Environment*, Vol. 95, No. 2, pp. 164–176. doi: 10.1016/j.rse.2004.12.011.